Indian Journal of Chemistry
Vol. 63, October 2024, pp. 1008-1014
DOI: 10.56042/ijc.v63i10.12665

# Preparation of ZnO/CuO under the regulation of SDS and its application in photocatalytic degradation

Aimin Ding, Wenqing Tai, Yijing Yuan, Tingting Zhang, Mengting Yan, Hongying Li* & Chengli Yao*

School of Pharmaceutical and Chemical Engineering, Hefei Normal University, Hefei 230601, P. R. China

E-mail: lhy@ustc.edu; yaochengli@hfnu.edu.cn

*Received 22 July 2024; accepted (revised) 20 September 2024*

As a green and efficient treatment technology, photocatalysis has enormous advantages in degrading organic pollutants in water. Here, zinc acetate, copper acetate, and sodium hydroxide have been used as raw materials to prepare ZnO/CuO composites under the mediation of sodium dodecyl sulfate (SDS). The structures and morphologies of desired products are characterized by X-ray powder diffraction (XRD) and scanning electron microscopy (SEM), respectively. The obtained samples used photo-catalysts to degrade the simulated pollutant of methylene blue (MB). The results show that the crystals of ZnO and CuO can be successfully produced with the co-precipitation method. Because of the regulation of SDS, the particles have high dispersibility and small particle sizes. Through photocatalytic performances, it is concluded that the degradation rate of the ZnO/CuO composite is higher than the corresponding monomers. It indicates that the synergistic effect of ZnO and CuO enhances the photocatalytic degradation ability of ZnO/CuO composite, providing a potential application prospect for the development of efficient photocatalysts for environmental governance.

**Keywords**: Copper oxide, Zinc oxide, ZnO/CuO composite, Photocatalysis, Surfactant

With the acceleration of modern urbanization, environmental pollution has gradually affected human health, and water pollution is one of the main problems[1,2]. The industries of textile, leather, paint, paper, plastic, and dyeing discharged toxic substances into water bodies, which were not easily degraded and reduced water quality. In particular, textile dyes caused more severe water pollution[3]. The method of traditional sewage treatment was difficult to meet the demand for wastewater purification. So, it is urgent to choose the appropriate sewage treatment method.

In recent years, physical, chemical, and biological methods have been used to remove organic dyes. Comparing the results, it was found that chemical methods were more effective than physical and biological methods[4]. It was worth mentioning that the treatment of photo-degradation had a broad prospect for applications[5]. Photocatalytic oxidation technology is the process of using photo-catalysts to oxidize and decompose pollutants in wastewater under light conditions. It can fully mineralize organic matter and ultimately convert them into non-toxic and harmless substances of $H_2O$, $CO_2$, and other inorganic small molecules. In general, photo-catalysts will be stimulated to generate electron-hole pairs under the irradiation of light with a certain wavelength. Then, electrons reduce oxygen atoms to active ions, and holes will decompose the surface of the photo-catalytic material to produce hydrogen and oxygen free radicals in the adsorbed water. Therefore, the photo-catalytic material has the function of oxidation-reduction degradation of pollutants[6,7]. Up to now, many photo-catalysts have been developed, such as $TiO_2$[8], $Cu_2O$[9], CdS[10], ZnS[11], Ag-based semiconductors[12]. Zinc oxide (ZnO) is a typical n-type semiconductor material with a wide bandgap of 3.37 eV. After absorbing ultraviolet light, it can generate electron-hole pairs to degrade organic and inorganic pollutants. Moreover, it has the advantages of environmental friendliness, low cost, high efficiency, and high electron mobility. However, there are still certain issues with semiconductor photo-catalytic technology at present, such as the fact that most semiconductor materials absorb the light with wavelengths less than 378 nm, which affects their practical application in production. In addition, the generated electron-hole pairs are easy to recombine, which has a significant impact on the photo-catalytic properties of ZnO. Therefore, people adopted methods such as dye sensitization of photo-catalytic substances, deposition and doping of precious metals, and composite photo-catalytic substances to solve the aforementioned problems[13,14]. For example, Samal

*et al.*[15] used a non-conventional method to synthesize ZnO-$SnO_2$ nanocomposites in a greener way, which improved the degradation efficiency of pollutants. In addition, the results of some research showed that composites of ZnO/$TiO_2$[16] and $WO_3$/$TiO_2$[17] could enhance the catalytic efficiencies. The semiconductor of CuO is an important p-type semiconductor with a narrow band gap (1.7 ev), as well as the advantages of good thermal stability, high electrochemical activity, and non-toxic[18]. It is applied in many fields, such as electronics, optoelectronics, sensors and gas sensors, heterogeneous catalysis, and solar cells.

During constructing the particles of ZnO and CuO with special structures and unique performances, template and hydrothermal methods were often selected. Among them, the former method was a relatively easy way to regulate the crystallization of ZnO and CuO[19-22]. For example, He and co-workers[23] used waste eggshell membranes as templates to synthesize CuO-ZnO composites. The results showed that the morphologies and structures of composites were regulated by the network of eggshell membranes and the prepared products exhibited excellent adsorption, catalysis, and antibacterial activities. Moreover, CuO and ZnO particles which were prepared by a biological template of Camellia japonica leaf extracts showed the optical sensing of metal ions and could be used as optical sensors for the detection of metal ions[24]. Surfactant was a common template. At a certain concentration, surfactant molecules self-assemble into capsules or micelles with unique structure, which could be used to induce the formation of ZnO and CuO crystals with specific structures and morphology. According to the interface theory of surfactants, it was easy to control the morphology and particle size of ZnO and CuO particles with desired performance by changing the composition and concentration of surfactant molecules to form expected vesicles or micelles.

Here, sodium dodecyl sulfate (SDS) was used as a control agent to prepare ZnO/CuO. A certain amounts of SDS were added during the preparation of desired products. At the same time, a binary photo-catalytic material of ZnO/CuO was prepared by combining the two precipitations. Subsequently, the morphology and structure of the obtained samples were characterized. Methylene blue (MB) served as the target pollutant to explore the photocatalytic abilities of samples. When the absorbed photon energy equals to or exceeds the band gap of CuO and ZnO under the light irradiation, electrons in the valence bands will be excited and transition to the conduction bands, while holes remain in the valence bands. Next, photo-generated electrons migrate from the conduction bands of CuO to ZnO, as well as photo-generated holes migrate from the valence bands of ZnO to CuO. This is due to the built-in electric field in the p-n junction between CuO and ZnO, which promotes the separation of photo-generated electron-hole pairs and suppresses carrier recombination. The desired products will show the enhanced photocatalytic degradation ability.

## Experimental Section

### Chemicals

Anhydrous zinc acetate ($Zn(Ac)_2$, AR), sodium dodecyl sulfate ($C1_2H_{25}SO_4Na$), anhydrous copper acetate ($Cu(Ac)_2$, AR), sodium hydroxide (NaOH, AR), methylene blue ($C_{16}H_{18}NClS$). Deionized water was used in whole experiments.

### Preparation of ZnO

50 mL of $Zn(Ac)_2$ solution (0.2 mol/L) were placed in a 500 mL beaker. Slowly dripped 200 mL of NaOH solution (0.1mol/L) into it, then the mixtures were stirred with magnetic force for 30 min. After the reaction was complete, let the mixture sit overnight. The precipitations were centrifuged, washed, collected, and dried under a vacuum at 60. Finally, the obtained solids were heated at 300 °C for 3h in a muffle furnace to prepare the ZnO samples. Finally, the desired products were prepared and named as **ZnO-1**. The main preparation process of ZnO under the regulation of SDS was the same as before, only adding 1.5 g of SDS solid during the synthesis process. The concentration and volume of reactants remained unchanged. Only the reaction temperature was set as 60°C. Then, the obtained products were named as **ZnO-2**.

### Preparation of CuO

50 mL of $Cu(Ac)_2$ solution (0.2 mol/L) and 200 mL of NaOH solution (0.1mol/L) were mixed, stirred magnetically for 30 minutes, and then let stand overnight. After the corresponding centrifugation, washing, and drying as described in the above step, the precipitations were collected and labeled as **CuO-1**. To prepare **CuO-2**, 1.5 g of SDS was selected to mediate the formation of CuO, which was added to the mixture of $Cu(Ac)_2$ and NaOH solution. After that, it was stirred magnetically at 60°C for 30

minutes. The dried precipitate was calcined at 300 °C in a muffle furnace to obtain a black powder solid of **CuO-2.**

**Preparation of ZnO/CuO**

50 mL of $Zn(Ac)_2$ solution (0.2 mol/L) and 50 mL of $Cu(Ac)_2$ solution (0.2 mol/L) were selected and mixed. 1.5 g of SDS powders was added to the mixture. After that, 400 mL of NaOH solution (0.1 mol/L) was added slowly stirring magnetically at 60 °C for 30 minutes. Then let it stand overnight. Referred to the aforementioned steps, the precipitations were centrifugated, dried, and calcined. Next, the target product of **ZnO/CuO** was obtained.

**Characterization of Samples**

The structures and morphologies of samples were characterized by X-ray powder diffraction (XRD, TF-5500, China) and scanning electron microscopy (SEM, SU-1510, Japan), respectively. The testing parameters of XRD analysis were set as Cu-Kα radiation (λ=1.54056 Å), scanning range of 2θ=10~80°, and scanning speed of 5°/min. Before the test of SEM, the trace-tested samples were dispersed in a certain volume of anhydrous ethanol, then dropped the dispersed solution was onto the silicon substrate and dried it. After completing the gold plating test, the morphologies of samples were observed by SEM.

**Photocatalytic degradation experiment**

$3.0\times10^{-5}$mol/L of methylene blue (MB) solution was served as a simulated pollutant. Adding photocatalysts (150 mg) to MB solution (150 mL), the dispersion was experienced sonication for 30 min to fully disperse the photocatalysts in the simulated pollutant under the dark condition. Afterwards, the dispersion was transferred to a photochemical apparatus (YM-GHX-VI, China) which was equipped with a 500 W xenon lamp as simulated sunlight. To allow it to continuously shine on the solution, the distance between the solution and the xenon was adjusted, and then the light was turned on. At regular intervals, 500 μL of degradation solution was taken out from the catalytic system, as well as added an equal volume of deionized water. The above operations were repeated until the blue color of the solution completely faded. The degradation solution was labeled sequentially. After high-speed centrifugation, the absorbance values of the supernatant were measured at a wavelength of λ=664 nm by a UV-visible spectrophotometer (UV-2550, Shimadzu). During degradation experiments, only the photocatalysts were changed. The degradation rates of each catalyst were calculated using equation (1) [25]. According to the degradation rates, a degradation curve was plotted.

$$\eta=\frac{(C_0-C_t)}{C_0}\times100\%=\frac{(A_0-A_t)}{A_0}\times100\%. \quad \text{... (1)}$$

where, η was the degradation rate of MB solution, and $C_x$(x=0, t) and $A_x$(x=0, t) were the concentration and absorbance of MB solution at time 0 and t, respectively.

**Results and Discussion**

Fig. 1 showed the XRD patterns of samples. From Fig. 1a, it could be seen that diffraction peaks were located at 2θ=31.8°, 34.4°, 36.3°, 47.5°, 56.6°, 62.9°, 66.4°, 68.0°, 69.1°, 72.6° and 77.0°. Compared with the standard card (JCPDF: No.79-0208), these diffraction peaks matched with (100), (002), (101), (102), (110), (103), (200), (112), (201), (004) and (202) crystal planes of ZnO, respectively, indicating that the structure was hexagonal wurtzite[26]. The appearance of characteristic diffraction peaks at 31.8°, 34.4°, and 36.3° further demonstrated the successful preparation of ZnO. The characteristic diffraction peaks appearing at 2θ=35.5°, 38.6° and 38.9° in Fig. 1b corresponded to the (110), (111) and (200) crystal planes of CuO (JCPDF: No.80-1916), respectively[27]. It demonstrated the successful preparation of CuO. Fig. 1c was the XRD pattern of the ZnO/CuO composite, from which it was easy to find the characteristic diffraction peaks of ZnO and CuO (the corresponding icons in Fig. 1c showed their respective positions) [28]. The sharp peak shape indicated good crystallinity of the solid crystal.

The SEM images of samples were shown in Fig. 2. The products of ZnO-1 (Fig. 2a) were large particles with irregular morphologies, which were prepared directly by the interaction of $Zn^{2+}$and $OH^-$ ions. The classical hexagonal feature was not found. This was due to the influence of various factors such as temperature, reactant concentration, and system composition on the morphologies of crystal particles. After the mediation of SDS, the crystal of ZnO-2 (Fig. 2b) showed disorderly, flocculent, and tightly clustered together.

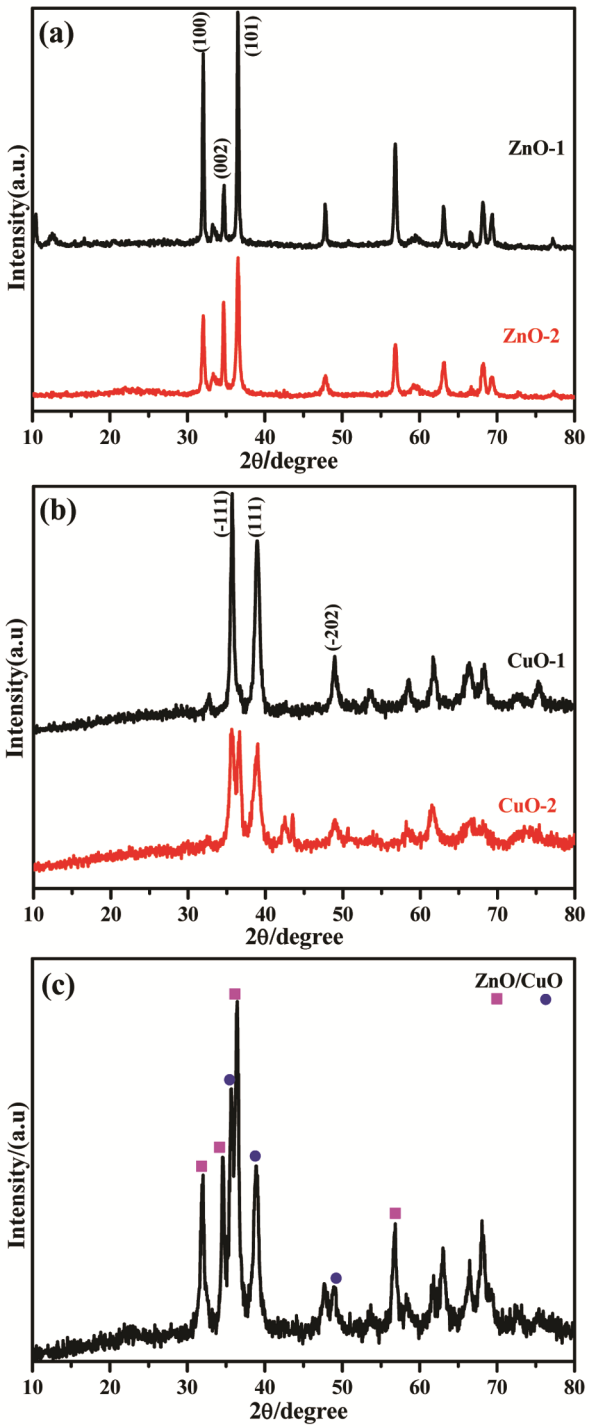


Fig. 1 — XRD patterns: ZnO-1 and ZnO-2(a), CuO-1and CuO-2(b), ZnO/CuO(c)

Under the control of SDS, the crystallization behaviorand mode of ZnO-2 were regulated and limited, and the particle size was significantly reduced and homogenized. The nanoscale size endowed ZnO samples with a larger specific surface area. Figs. 2c-d

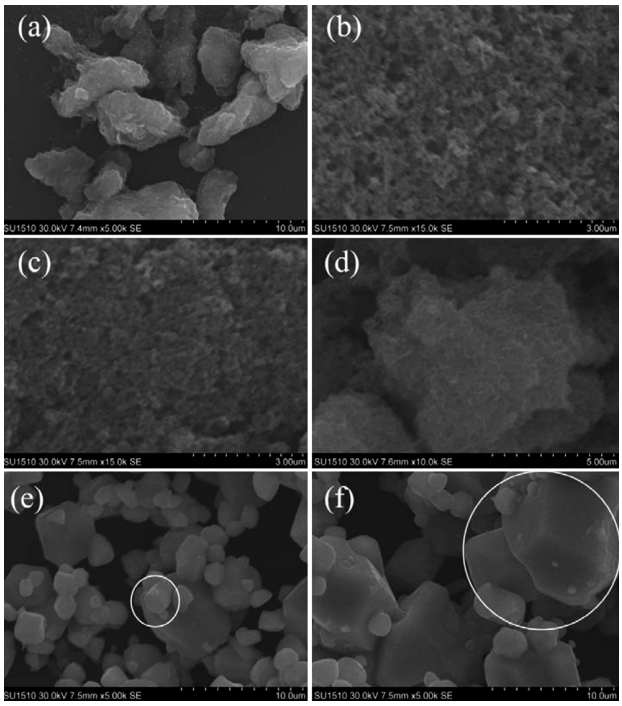


Fig. 2 — SEM images: ZnO-1(a), ZnO-2(b), CuO-1(c), CuO-2(d), ZnO/CuO(e,f)

were SEM images of CuO-1 and CuO-2, respectively. The former was a nanoscale rod-shaped, while the latter was a layered aggregation. Nanoparticles were endowed with certain advantages in photocatalysis. Figs. 2e-f showed the SEM images of the ZnO/CuO composite induced by SDS. The particles in the figure were dispersed, and hexagonal columnar ZnO crystals (circled in Fig. 2e) and polyhedral CuO particles (circled in Fig. 2f) could be observed from them.

In order to evaluate the photocatalytic performance of the prepared samples, the absorbance values of MB solution at the wavelength of λ=665 nm under the action of catalysts were detected by a UV-visible spectrophotometer. The spectra were shown in Fig. 3. Overall, the absorbance values of the solution continuously decreased, indicating a gradual weakening of MB absorption. From Fig. 3, it could be found that the decreased rate of absorbance values of MB at the maximum absorption wavelength was related to the type of catalysts. Specifically, under the degradation of ZnO-2 took 48 min to decrease the absorbance values of the solution from 1.6 to 0.5 (Fig. 3b), while ZnO-1 was 70 min (Fig. 3a). For CuO-1 (Fig. 3c) and CuO-2 (Fig. 3d), after 70 min of degradation, the absorbance value of MB solution remained at 0.8. Unlike the monomers of ZnO and CuO, the composite ZnO/CuO (Fig. 3e) exhibited a

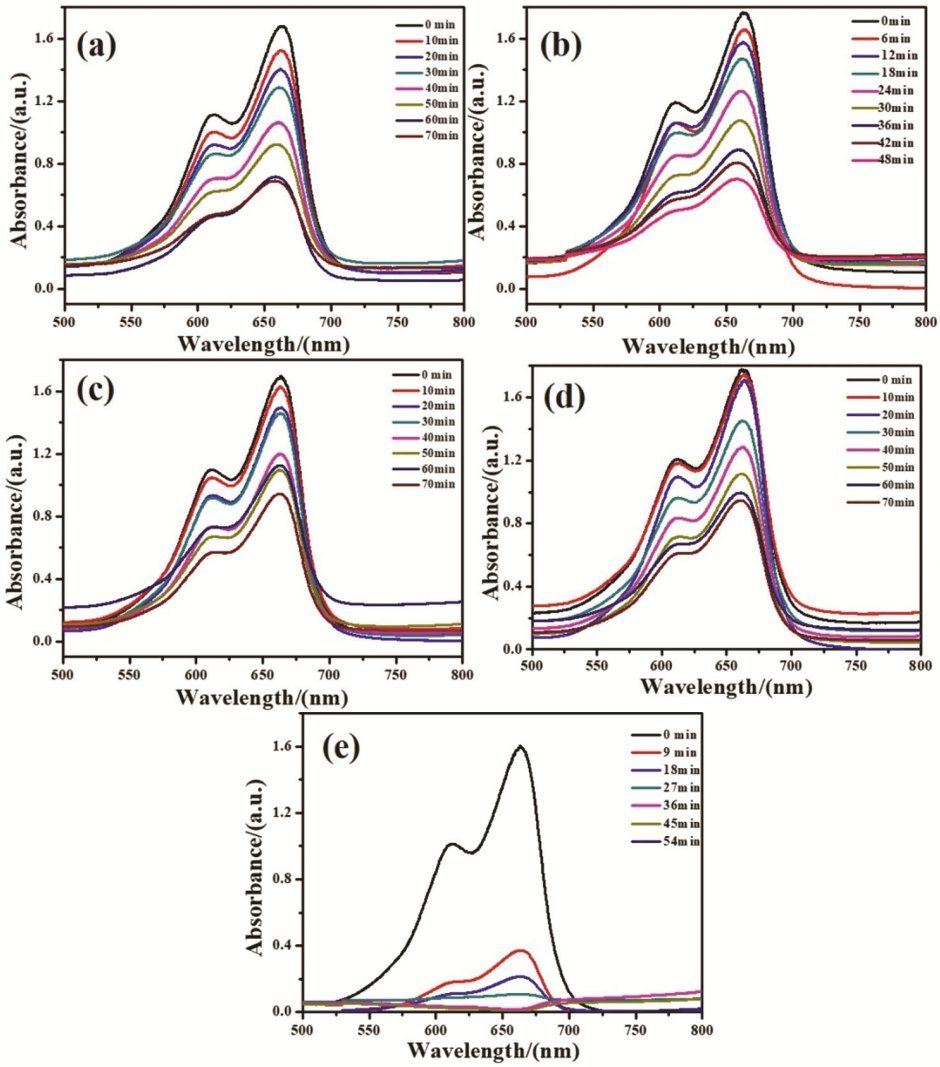


Fig. 3 — The UV-Vis spectra of methylene blue solution catalyzed by: ZnO-1(a), ZnO-2(b), CuO-1(c), CuO-2(d), ZnO/CuO(e)

significant catalytic degradation effect, and the UV absorption peak of MB disappeared after about 30 min.

To compare the degradation effects of catalysts more intuitively, the corresponding efficiency at different times according to formula (1) was calculated, and the curves were drawn (Fig. 4). It was easy to find that the composite catalyst of ZnO/CuO showed an obviously photocatalytic property with a degradation rate of nearly 85% after about 30 min, while the catalytic efficiency of other monomer catalyst was below 40% under the same conditions. Except for ZnO-2, the degradation efficiency of the other three monomer catalysts did not reach 60% during a continuous 60 min irradiation. For monomers, ZnO-2 was superior to ZnO-1, while the effect of CuO-1 and CuO-2 was of no significant difference.

Due to the very low concentration of MB in the experiments ($3.0\times10^{-5}$mol/L), the photocatalyticde gradation process could be considered to follow the pseudo-first-order kinetics[29]. Therefore, according to equation (2), the rate constants of degradation reactions were linearly fitted and calculated, and kinetic curves were drawn and shown in Fig. 5.

$$\ln\frac{C_0}{C_t}=\ln\frac{A_0}{A_t}=kt \quad \text{... (2)}$$

Among them, k and t represented the rate constant and photocatalytic degradation time, respectively.

Based on the fitting results of degradation kinetics curves for each catalyst, Table 1 was illustrated. Based on the degradation rate curve, fit the obtained kinetic curve as shown in Fig. 5, and extract relevant data to draw Table 1. It was easy to obtain from

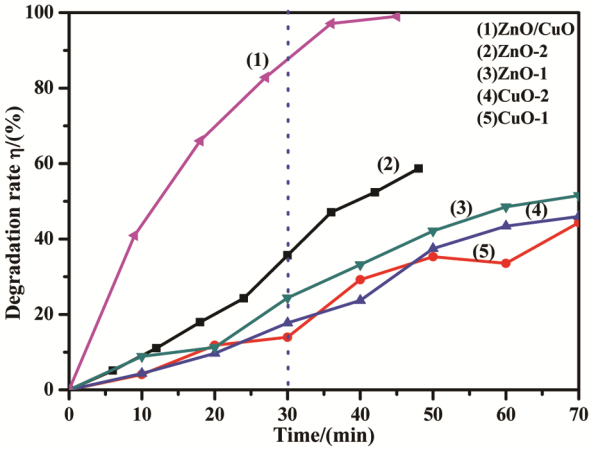


Fig. 4 — Degradation Rate Curves

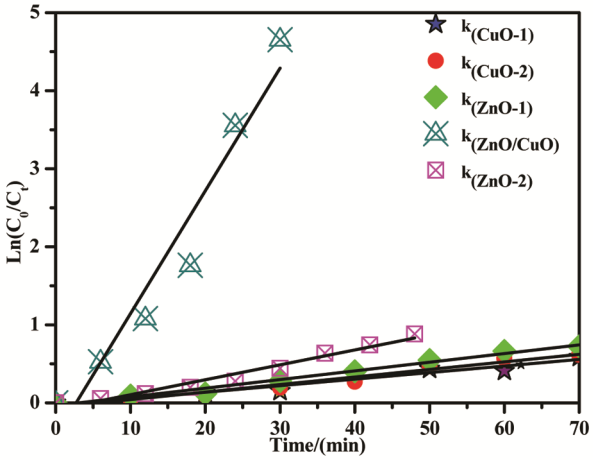


Fig. 5 — Kinetic Curves

Table 1 — Kinetic Curve Parameters

| Catalysts | Rate constants($k$/min$^{-1}$) | $R^2$ |
|---|---|---|
| ZnO-1 | 0.01111 | 0.98097 |
| ZnO-2 | 0.01912 | 0.96112 |
| CuO-1 | 0.00841 | 0.94381 |
| CuO-2 | 0.00967 | 0.96109 |
| ZnO/CuO | 0.15733 | 0.93093 |

Table 1 that the relationship of the reaction rate constants was $k_{ZnO/CuO}>k_{ZnO-2}>k_{ZnO-1}>k_{CuO-2}>k_{CuO-1}$. $k_{ZnO/CuO}$was significantly larger than the k values of each monomer, which was 8 and 16 times higher than $k_{ZnO-2}$ and $k_{CuO-2}$, respectively.

In summary, the prepared samples in this study all have certain catalytic degradation properties, but the differences in composition and structure determined the inconsistent degradation ability. Among the monomeric catalysts, the ZnO series are significantly better than the CuO series, which may be due to the narrow band gap of CuO during the capture of photons by semiconductors, which is not conducive to electron transfer, resulting in a lower catalytic ability than the wide band gap of ZnO[30-31]. In addition, due to the regulation of SDS, the prepared ZnO-2 and CuO-2 have high dispersibility and small particle sizes, which gives these particles greater specific surface area and more opportunities to adsorb methylene blue molecules. The excellent degradation ability of the composite ZnO/CuO may be related to the following factors: (1) The regulation of SDS leads to good product dispersion; (2) Due to the strong absorption of visible light, the addition of narrow band gap semiconductor CuO is beneficial to the redshift of the light absorption boundary of CuO/ZnO, increasing the light absorption range and efficiency of the sample. So, the recombination of photo-generated electron-hole pairs is inhibited, the recombination rate of photo-generated electrons and holes is reduced, more visible light is absorbed to stimulate more photo-generated carriers, and the degradation of organic pollutants under visible light is enhanced[32-34].

## Conclusion

The photocatalytic material of the ZnO/CuOcomposite was synthesized with the co-precipitation method using SDS as a regulator. Under the control of SDS, the dispersion of the ZnO/CuO composite was good, and the intrinsic morphology was obvious. Taking methylene blue as the pollutant, the composite ZnO/CuO exhibited excellent photocatalytic degradation ability under the simulated sunlight irradiation, which was significantly higher than that of each monomer, indicating that the photocatalytic material of ZnO/CuO showed a certain synergistic effect. Under irradiation, CuO and ZnO were excited to produce electron-hole pairs. At the same time, the recombination rate was reduced, promoting their separation, the carrier recombination was suppressed, and thus the utilization efficiency of light was improved. The preparation of composite catalyst ZnO/CuO provided an effective approach for the rational utilization of the catalytic performance of each monomer and the full utilization of raw materials.

## Acknowledgment

This work is supported by Natural Science Foundation of the Department of Education of Anhui Province (2022AH052139, 2024AH051555), Anhui

Province Young Teacher Training Action: Discipline (Major) Leader Cultivation Project (Grant No. DTR2023037), and Research Project of Hefei Normal University (HXXM2023120, HXXM2023131).

## References


1 Wang W, Lv Y, Liu H & Cao Z, *Sep Purif Tech*, 330 (2024) 125265.
2 Chen Z, He G, You T, Zhang T, Liu B & Wang Y, *J Env Chem Eng*, 12 (2024) 112191.
3 Rafiq A, Ikram M, Ali S, Niaz F, Khan M, Khan Q & Maqbool M, *J Ind Eng Chem*, 97 (2021) 111.
4 Kedruk Y, Baigarinova G, Gritsenko L, Cicero G & Abdullin K, *Front Mater*, 9 (2022) 869493.
5 Lanjwani M, Tuzen M, Khuhawar M & Saleh T, *InorgChemComm*, 159 (2024) 111613.
6 Bhapkar A &Bhame S, *J Env Chem Eng*, 12 (2024) 112553.
7 Imran M, Raza M, H Noor H, Faraz S, Raza A, Farooq U, Khan M, Ali S, Bakather Y, Ali W, Bashiri A & Zakri W, *Chemosphere*, 359 (2024) 142224.
8 Baamer D, Helmy E, Mostafa M & Pan J*, Ceram Int*, 50 (2024) 15780
9 Zhang Y, Zhang Z, Zhang Y, Li Y & Yuan Y, *J Coll Int Sci*, 651 (2023) 117.
10 Zhang Q, Luo W, Yang T, Li R, Gao Q, Cai X, Zhang S, Fang Y, Zhou X, Peng F & Yang S, *Sep Purif Tech*, 346 (2024) 127391.
11 Khan M &Abdulwahab K, *Mat Sci Semicon Proc*, 181 (2024) 108634.
12 Li G, Yang C, He Q & Liu J, *J Environ ChemEng*, 10 (2022) 107374.
13 Hareeshanaik S, Prabhakara M, BhojyaNaik H, Viswanath R, Shivaraj B, Vishnu G & Adarshgowda N, *Inorg Chem Comm*, 158 (2023) 111552.
14 Qiu Y, Fan H, Tan G, Yang M, Yang X & Yang S, *Mater Lett*,131 (2014) 64.
15 Samal A, Pouthika K, Rajesh A, Roopan S & Madhumitha G, *Inorg Chem Comm*, 159 (204) 111809.
16 Nie C, Liu L & He R, *Sep Purif Tech*, 206 (2018) 316.
17 Zhang Y, Liu D, Xiong B, Li J, Li Y, Zhou Y, Yang A & Zhang Q, *Solid State Sci*, 131 (2022) 106963.
18 Chen Y, Bagnall D, Koh H, Park K, Hiraga K, Zhu Z & Yao T, *J ApplPhys*, 184 (1998) 3912.
19 Yang S, Wang J, Liu L, Ren P, Yang Q & Zhao G, *Ceram Int*, 47 (2021) 8610.
20 Hu Y, Sun L, Liu Z & Liu T, *Mater Chem Phys*, 299 (2023) 127525.
21 Zou Y, YLi Y, Guo Y, Zhou Q &An D, *Mater Res Bull*, 47 (2012) 3135.
22 Nogueira A, Giroto A, Neto A &Ribeiro C, *Colloid Surface A*, 498 (2016) 161.
23 He X,Yang D, Zhang X, Liu M, Kang Z, Lin C, Jia N & Luque R, *Chem Eng J*, 369 (2019) 621.
24 Maruthupandy M, Zuo Y, Chen J, Song J, Niu H, Mao C, Zhang S & Shen Y, *Appl Surf Sci*, 397 (2017) 167.
25 Li H, Liu X, Huang J, Zhu W, Ding A & Yao C, *Crystallogr Rep*, 67 (2022) 123.
26 Gupta K, Sharma B, Garg V, Neelratan P, Kumar V, Kumar D & Sharma S, *Hybrid Adv*, 5 (2024) 100160.
27 Nouren S, Bibi I, Kausar A, Sultan M, Bhatti H, Safa Y, Sadaf S, Alwadai N & Iqbal M, *J King Saud Univ Sci*, 36 (2024) 103089.
28 Pandey P &Choubey A, *J Alloy Compd*, 970 (2024) 172492.
29 Yao C, Chen C, Yuan Y, Zhu W, Tai W, Ding C & Li H, *Cryst Res Tech*, 59 (2024) 2300233.
30 Xie L, Wang P, Li Z, Liu D & Wu Y, *Chinese J Mat Res*, 33 (2019) 728.
31 Mrabet C, Jaballah R, Mahdhi N, Boukhachem A &Amlouk M, *J Alloy Comp*, 968 (2023) 172252.
32 Mubeen K, Irshad A, Safeen A, Aziz U, Safeen K, Ghani T, Khan K, Ali Z &Haq I, Shah A, *J Saudi ChemSoc*, 27 (2023) 101639.
33 Yousefinia A, Khodadadi M &Mortazavi-Derazkola S, *Env Tech Inn*, 32 (2023) 103340.
34 Długosz O, Wąsowicz N, Szostak K & Banach M, *Mat Chem Phys*, 260 (2021) 124150.